Structure Determination of Enalapril Maleate Form II from High-Resolution X-ray Powder Diffraction Data

Y.-H. Kiang*[†], Ashfia Huq[‡], Peter W. Stephens[‡], Wei Xu[†]

† Pharmaceutical Research and Development, Merck Research Laboratories,

Merck & Co., Inc., P.O. Box 4, West Point, PA, 19426

‡ Department of Physics and Astronomy, State University of New York,

Stony Brook, NY, 11794

Accepted

Journal of Pharmaceutical Sciences

March 5, 2003

*Author to whom correspondence should be addressed. (yuanhon_kiang@merck.com)

Abstract

The crystal structure of polymorphic form II of enalapril maleate, a potent angiotensin converting enzyme (ACE) inhibitor, was determined from high-resolution X-ray diffraction data using the direct space method. Enalapril maleate Form II crystallizes in space group $P2_12_12_1$, Z=4, with unit cell parameters a=33.9898(3), b=11.2109, c=6.64195(7) Å, and V=2530.96(5) Å^3. By treating the molecules as rigid bodies and using the bond lengths and angles obtained from the X-ray single crystal structures of Form I, which were solved almost 20 years ago, the total degrees of freedom of enalapril maleate were reduced from 25 to 12. This reduction in total degrees of freedom allowed the simulated annealing to complete within a reasonable computation time. In the crystal structure of Form II, the crystal packing, hydrogen-bonding pattern, and conformation of enalapril maleate resemble those in the structure of Form I. The crystal packing and conformation of enalapril maleate in the two polymorphic forms may explain the similarity of thethermal properties, ^{13}C-NMR, FT-IR, and Raman spectra of Form I and II. In both structures, the conformations of the main peptide chains, which are considered responsible for binding the active ACE sites, remain largely unchanged. Lattice energy calculation showed that Form II is slightly more stable than Form I by 3.5 kcal/mole.

Keywords: enalapril maleate, polymorphism, crystal structure determination, X-ray powder diffraction (XRPD) pattern, Monte-Carlo/Simulated Annealing

Introduction

Since the development of captopril and enalapril,[1-2] angiotensin converting enzyme (ACE) inhibitors have attracted much attention for their applications in control of hypertension. X-ray single crystal structures of many ACE inhibitors have been determined and the conformations analyzed in attempt to use the results as an aid in the design of new ACE inhibitors.[3-12] The X-ray single crystal structure of enalapril maleate Form I was solved and reported by two independent groups in 1986.[3-4] The reported structures were since used in a number of research papers to provide conformational information of the enalapril molecule in solid state.[3-4,12-13] Enalapril maleate, however, exists in another polymorphic form denoted as Form II,[14] the structure of which has not been reported to date.

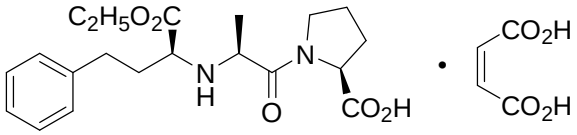

Polymorphism, the existence of two or more crystal forms of the same compound, is very common in pharmaceutical solids.[15-16] Characterization and control of polymorphism has been of particular importance to the pharmaceutical industry as change of polymorphs can alter the bulk properties, bioavailability, and the chemical and physical stability of a drug. The fundamental understanding of polymorphism comes from the knowledge of crystal structure at the atomic level. However, determination of crystal structure is often challenging due to the difficulty of growing single crystals suitable for X-ray analysis. Polymorphs are therefore routinely identified using X-ray powder diffraction patterns and the structural information is obtained indirectly from XRPD, solid state NMR, IR and Raman. In the case of enalapril maleate, two polymorphic forms were reported in 1986 by Ip and co-workers using spectroscopic data and solution calorimetry.[14] The XRPD patterns and solid state ^{13}C NMR spectra of these two polymorphs are shown in Figure 1 and 2, respectively. Based on the spectroscopic data, the two polymorphs of enalapril maleate are concluded to be very similar in their structures. However, the X-ray single crystal structure of the Form II has never been obtained and probably will never be as the Form II is made from water slurry of Form I.

In the aforementioned research papers of ACE inhibitors, the conformational information of enalapril was taken from Form I, the only known crystal structure. A crystal structure solution of the Form II will therefore provide clearer understanding of the polymorphism of enalapril maleate as well as more complete information on the enalapril conformation in the solid state.

Crystal structure determination based on XRPD patterns using the direct space method has become increasingly important for pharmaceutical solids with the increasing use of high resolution x-ray diffraction data, the development of new computer programs, and improved search algorithms.[17-19] In the past 5 years, more than 10 crystal structures of pharmaceutical solids have been determined based on X-ray powder diffraction patterns.[20-24] Among the currently available search algorithms for direct space method, Monte-Carlo/Simulated Annealing (MC/SA) has been most widely used.[25-28] This search algorithm employs random sampling coupled with simulated temperature annealing in order to locate the global minimum of the figure-of-merit factor. As the computing time increases exponentially with the increase of total degrees of freedom, size of the system is critical to the success of the MC/SA search. When MC/SA is used in the direct space method for solving crystal structures from powder diffraction data, large flexible molecules or salts with counter ions are usually considered non-favorable because of the higher total degrees of freedom. Nonetheless, prior experimental knowledge on the molecules from single crystal structures of other polymorphs sometimes may be useful to reduce the total degrees of freedom. For a complete structure determination, the structural solution obtained form MC/SA should be subsequently subject to refinement for the atomic positions and thermal factors.

In this work we report the crystal structure of enalapril maleate Form II from high-resolution synchrotron X-ray powder diffraction data. The structural solution was obtained using a MC/SA search algorithm and the atom positions were refined individually. The crystal packing of Form II and I was analyzed and the analysis was used to understand the solid state ^{13}C NMR and IR spectra of the two forms. The molecular conformation of enalapril in Form II was compared to the one in the Form I

crystal structure. The crystal structures were also used to calculate the lattice energies of the two polymorphic forms.

Experimental Section

General Procedure: The polymorphic Form II of enalapril maleate ((S)-1-[N-[1-(ethoxycarbonyl)-3-phenylpropyl-L-analyl]-L-proline maleate) was obtained from Merck & Co., Inc. (>98% purity), and used without further recrystallization. Slow evaporation of the methanol solution of enalapril maleate yielded Form I. The samples were sealed in 0.7mm special glass capillary tubes, and powder X-ray diffraction data were collected on an Inel MPD X-ray diffractometer equipped with a CPS 120 detector at 35 kV, 30 mA, for Cu $K_{\alpha 1}$ (λ =1.5406Å) monochromated by a Germanium(111) crystal. A mixture of silicon and silver behenate was used as an external standard.

Synchrotron X-ray diffraction measurement was performed on beam-line X3B1 at the National Synchrotron Light Source, Brookhaven National Laboratory. The X-ray wavelength of 1.1508Å was selected by double crystal Si(111) monochromator. The diffracted beam was selected using a Ge(111) analyzer and detected with a Na(Tl)I scintillation counter with a pulse-height discriminator in the counting chain. The diffracted intensity was normalized to the incident beam, monitored by an ion chamber. The powder sample was sealed in a 1.5 mm thin-wall glass capillary tube and X-ray diffraction data were recorded with a step size of 0.005º and a counting time 2 sec/step from 2º to 20º in 2θ, increasing quadratically to 17 sec/step at 47.65º. During data collection the sample was rotated to reduce the effect of sample granularity. The peaks were fitted by a local deconvolution program and powder data were indexed by the computer program ITO[29] into an orthorhombic cell, giving a figure of merit M(20) of 308. The systematic absences suggested $P2_12_12_1$ as a possible space group.

Infrared spectra were recorded on a Perkin Elmer FT-IR spectrometer Spectrum One using reflective mode: number of scans was 64; resolution was 1 cm^{-1}; range was 4000-400 cm^{-1}. High-resolution ^{13}C spectra were obtained by cross-polarization magic-angle spinning (CPMAS) experiments at 100.627 MHz on a Bruker DSX-400 WB NMR

spectrometer with a 7 mm H/X CPMAS probe. Approximately 200 mg of sample was placed in a Zirconia rotor sealed with Kel-F caps under ambient conditions and spun at 7 kHz during the experiment. Cross-polarization was done at Hartman-Hann condition. The contact time and the repetition delay were optimized to 2 ms and 5 s, respectively. The free induction decay was acquired for 50 ms; 4 K data points were collected and zero-filled to 8 K before transformation using 20 Hz of line broadening. For each form 600 scans were accumulated. Glycine resonance at 43.6 ppm was used as an external standard for chemical shift assignments referenced to TMS.

Structure Solution: The structure determination from the synchrotron X-ray powder diffraction pattern was carried out using the MC/SA program *PowderSolve*, which is incorporated in the molecular simulation package *Material Studio*.[30] The molecular models of the enalapril and maleate were obtained from the single crystal structure of the Form I and used without further optimization. For the MC/SA search algorithm, the total degrees of freedom of the system is important to the success of the simulation. In the enalapril maleate system, the total degrees of freedom for enalapril is 17 (11 torsional, 3 translational, and 3 rotational), and for maleate is 8 (2 torsional, 3 translational, and 3 rotational). Although at the high end, the total 25 degrees of freedom were within the computation limit of current computers and MC/SA programs. However, trials with this many degrees of freedom using the two programs *PowderSolve* and *PSSP*[19] were not successful. Since the Form I single crystal structure was known and considered structurally similar to the Form II based on the XRD patterns and the ^{13}C NMR spectra, we tried to search a restricted space. Rigid molecular fragments of enalapril and maleate from the single crystal structure of Form I were used to start the MC/SA with all torsional degrees of freedom fixed. This approach reduced the total degrees of freedom from 25 to 12 and made the MC/SA search process for the Form II crystal structure much more rapid. The final *R*wp ($R\text{wp}=[\sum_i w_i|I_{\text{exp}}(\theta_i)-I_{\text{calc}}(\theta_i)|^2/\ \sum_i w_i|\ I_{\text{exp}}(\theta_i)|]^{1/2}$) from the first three cycles of MC/SA was 17.51%. The torsion angles of the enalapril molecule were then released to refine while the torsional degrees of freedom for the maleate molecules as well as the intermolecular degrees of freedom were fixed for the subsequent MC/SA

search. Three cycles of MC/SA search further reduced the *R*wp factor from 17.51% to 14.04%. An iterative process of selectively refining part of the total degrees of freedom resulted in a convergent final *R*wp factor of 13.66%, indicating the structural model was successfully located by the MC/SA search. This process is summarized in Table 1. The structural solution obtained from *PowderSolve* was subsequently used for Rietveld profile refinement with the program GSAS.[31]

In the Rietveld refinement the atomic positions of all non-hydrogen atoms were refined without any constraints. The overall temperature factors were refined to two numbers: one for the enalapril molecule and the other for the maleate molecule. The final *R*wp of the Rietveld refinement was 7.61%, indicating the reliability of the refinement. The experimental XRPD pattern, the powder pattern calculated for the fully refined structure, and the difference between the two patterns are shown in Figure 3. Table 2 lists the Rietveld refinement information and the crystal data of enalapril maleate Form II. The higher value of χ^2, 31.1, is due to the high counting statistics and the excellent signal-to-background ratio of the raw experiment data. The hydrogen atoms were included after the refinement at their geometrically constrained positions. The atomic coordinates and isotropic displacement parameters are listed in Table 3.

Results and Discussion

The crystal structure of enalapril maleate Form I is illustrated in Figure 4. In this structure there is only one crystallographically non-equivalent enalapril maleate molecule. After the symmetry operations of the space group, four enalapril maleate molecules were generated in the unit cell. The maleate molecule is found considerably deviated from planarity. This deviation is consistent with the maleate in the Form I single crystal structure and has to be attributed to hydrogen bonding and crystal packing effects. The single crystal structure of Form I indicated that the enalapril maleate molecule is protonated at the analyl N and this information is used in the Form II structure. Based on the distance between the alanyl nitrogen atom and one of the maleate oxygen atoms (2.76Å), the enalapril molecule is hydrogen bonded to the maleate through the protonated

alanyl nitrogen atom. An additional hydrogen bond links the analyl N atom to the carboxylate oxygen atom of an adjacent enalapril. These hydrogen bonded enalapril molecules are symmetrically related by a 2-fold screw axis along the *c* axis. Apart from these hydrogen bonds, all other intermolecular contacts correspond to normal van der Waals interactions.

The crystal packing of the two polymorphs is shown in Figure 5. In Figure 5, one sees that the two polymorphic forms of enalapril maleate are of very similar crystal packing pattern as expected from the spectroscopic data. The space group of Form I is $P2_1$. In $P2_1$ the only symmetry operation is a 2-fold axis along the *b* axis, which is pointing into the paper in Figure 5. All the enalapril maleate molecules in Form I are related to one another by this 2-fold screw axis. On the other hand, Form II is crystallized in $P2_12_12_1$, in which three 2-fold screw axes are present along *a*, *b*, and *c* directions. In both figure 5a and b, the eight enalapril maleate molecules can be divided into two groups each containing four molecules, the first group being at the top and the second group at the bottom of the figure. In the structure of Form II, within each group the four enalapril maleate molecules are related by a 2-fold screw axis along the *c* axis, which is pointing into the paper as the *b* axis in Form I. However, unlike the Form I structure, the two groups in Form II are related by a 2-fold screw axis along the *b* axis, which in Figure 5b is lying on the paper horizontally from left to right. The analyl carbonyl groups in Form I are all pointing into the paper; however, in the structure of Form II the analyl carbonyl groups in the first group are pointing out of the paper while in the second group they are pointing into the paper.

The main difference in crystal packing between the two polymorphs lies in the distance of the two phenyl rings of adjacent enalapril molecules. In Form I, the closest distance between the two phenyl rings is about 3.5Å and the farthest is 6.6Å, while in Form II the closest distance is 3.8Å and the farthest is 7.5Å. In both structures, based on the distance of the two phenyl rings, the interaction between the phenyl rings is considered weaker than normal π–π interaction. This difference in crystal packing of the two forms is also supported by the IR and ^{13}C solid-state NMR spectra. The IR (Figure 6)

spectra of the two forms are almost identical except in the region of 750 cm^{-1}, which is the region of an out-of-plane phenyl ring-hydrogen interaction. In the ^{13}C solid state NMR of the two forms shown in Figure 7 and 8, the main differences occur in the aromatic ring and methyl group regions. These NMR data are in agreement with what one sees in Figure 5, in which the phenyl ring stacking and the methyl group orientation are the main differences in the crystal packing.

The conformation of the enalapril maleate molecule in both crystal Form I and II along with the atom numbering are shown in Figure 9. The selected torsion angles of the two forms are summarized in Table 4. In Table 4 the torsion angles of the peptide chains are almost identical in the two structures. In standard nomenclature, the alanine peptide main chain is described by torsional angles $\phi 1$, $\psi 1$, and ω; the proline peptide chain is described by $\phi 2$ and $\psi 2$. In both structures, the observed rotamer around the proline is trans (ω close to -180°). At the alanine, the three torsion angles $\varphi 1$, $\psi 1$, and ω correspond to a nearly fully extended conformation. Two angles, ω and $\phi 2$, defining the spatial orientations of amide carbonyl and carboxy groups are restricted in the antiperiplanar and synclinal regions respectively. The selected torsion angles are listed in Table 5. It is noteworthy to find that the only difference in the enalapril conformations of the two polymorphs exists in the dihedral angle C15-O17-C18-C19 of the esterified carboxylate group. This dihedral angle was considered of no significance in defining the required conformation for ACE inhibitors. As a matter of fact, enalapril is the prodrug of its active form, enalaprilat, in which the ethyl ester group of enalapril is hydrolyzed. In the enzyme-ligand binding model, this hydrolyzed ester, the carboxyl group at C14, is the actual zinc-binding group. All the anchoring sites of enalapril in the two polymorphs therefore have almost identical torsion angles. The enalapril conformations determined in solid-state are also in agreement with the in-solution conformation determined based on NMR analyses.[13]

The similarity in the conformations of enalapril molecule in the two polymorphs supports the conclusion by Pascard and co-workers.[12] In their study, the crystal structures of six ACE inhibitors including hydrates and solvates were analyzed and found

to adopt similar conformations in the peptide chains. Since the similar conformations were found throughout different solvates and cell dimensions, Pascard concluded that the commonly observed conformation was likely due to an energy minimum rather than packing effect.

Finally, the crystal structures of the two polymorphic forms were used to calculate their packing energies.[32] In this calculation the force field "Dreiding 2.21" was used with the Ewald summation for both the van der Waals and Coulombic terms.[33] The force field "Dreiding 2.21" was chosen based on reports that the Dreiding force field can model structures with hydrogen bonds between C=O and N-H particularly well.[34-36] Since enalapril maleate is a charged salt, the Coulombic interaction is expected to contribute the most to the total energy of the crystal. The molecular electrostatic potential of enalapril maleate was therefore a deciding factor for the calculated energy and was obtained according to the restricted Hartree-Fock formalism (RHF) at the 6-31G** level with the quantum mechanic program Gaussian97.[37] The calculated lattice energies (at the temperature of 0 K) per asymmetric unit for Form I and II are -86.46 and -90.10 kcal/mole, respectively. Ip and co-workers have reported the heat of solutions for the two forms and showed that Form II is slightly more stable than Form I by 0.6 kcal/mole.[14] Our energy calculation showed that Form II is slightly more stable than Form I by 3.5 kcal/mol. This observation that Form II is slightly more stable than Form I may also be understood by the density rule. The densities of the two forms are 1.27 (Form I) and 1.29 (Form II) g/cm^3. The Kitaigorodskii closest packing model states that the basic factor that affects free energy is the packing density.[38] The denser or more closely packed crystal has the lower free energy. The crystal structures of the two forms were both solved at room temperature and in both structures only one crystallographically non-equivalent molecular pair was found. As Form II is slightly denser than Form I, it is expected that Form II is slightly more stable than Form I at room temperature based on the Kitaigordskii density theory.

Acknowledgments

The authors are grateful to Dr. Robert Wenslow and Mr. Russell Ferlita of Analytical Research, Merck & Co., Inc. for obtaining the solid state NMR data. We wish to thank Prof. Stephen Lee of Cornell University for use of his X-ray diffractometer. Research carried out in part at the National Synchrotron Light Source at Brookhaven National Laboratory, which is supported by the US Department of Energy, Division of Materials Sciences and Division of Chemical Sciences. The SUNY X3 beamline at NSLS is supported by the Division of Basic Energy Sciences of the US Department of Energy under Grant No. DE-FG02-86ER45231.

References:

1. Ondetti MA, Rubin, B, Cushman DW. 1977. Design of specific inhibitors of angiotensin-converting enzyme: new class of orally active antihypertensive agents. Science 196:441-444.
2. Patchett AA, Harris E, Tristram EW, Wyvratt MJ, Wu MT, Taub D, Peterson ER, Ikeler TJ, ten Broeke J, Payne LG, Ondeyka DL, Thorsett ED, Greenlee WJ, Lohr NS, Hoffsommer RD, Joshua H, Ruyle WV, Rothrock JW, Aster SD, Maycock AL, Robinson FM, Hirschmann R, Sweet CS, Ulm EH, Gross DM, Vassil TC, Stone CA. 1980. A new class of angiotensin-converting enzyme inhibitors. Nature 288:280-283.
3. Fujinaga M, James MNG. 1980. SQ 14,225:1-(D-3-mercapto-2-methylpropionyl)L-proline. Acta Crystallogr B36:3196-3199.
4. Précigoux G, Geoffre S, Leroy F. 1986. N-(1-Ethoxycarbonyl-3-phenylpropyl)-L-alanyl-L-prolinium-hydrogen maleate (1/1), enalapril (MK-421). Acta Crystallogr C42:1022-1024.
5. In Y, Shibata M, Doi M, Ishida T, Inoue M, Sasaki Y, Morimoto S. 1986. Conformational similarities of angiotensin-converting enzyme inhibitors: X-ray crystal structures. Chem Commun 473-474.
6. Wyvratt M, Tristram EW, Ikeler TJ, Lohr NS, Joshua H, Springer JP, Byron HA, Patchett AA. 1984. Reductive amination of ethyl 2-oxo-4-phenylbutamoate with L-alanyl-L-proline. Synthesis of enalapril maleate. J Org Chem 49:2816-2819.
7. Paulus EF, Hennings R, Urbach H. 1987. Structure of the angiotensin-converting enzyme inhibitor ramiprilat (HOE 498 diacid). Acta Crystallogr C43:941-5.
8. Luger P, Schnorrenberg G. 1987. A highly potent angiotension converting enzyme inhibitor: (S,S,S)-5-[N-(1-carboxy-3-phenylpropyl)alanyl]-4,5,6,7-tetrahydrothieno[3,2-c]pyridine-4-carboxylic acid monohydrate, SBG 107. Acta Crystallogr C43:484-8.
9. Attwood MR, Francis RJ. 1984. New potent inhibitors of angiotensin converting enzyme. FERB Lett 165:201-206.
10. Attwood MR, Hassall CH, Krohn A, Lawton G, Redshaw SJ. Chem Soc, Perkin Trans 1 1011-19.
11. Thorsett ED, Harris EE, Aster SD, Peterson ER, Synder JP, Springer JP, Hirshfield J, Tristram EW, Patchett AA, Ulm EH, Vassil TC. 1986. Conformationally restricted

inhibitors of angiotensin converting enzyme: Synthesis and computations. J Med Chem 29:251-260.

12. Pascard C, Guilhem J, Vincent M, Rémond G, Portevin B, Laubie M. 1991. Configuration and preferential solid-state conformations of perindoprilat (S-9780). Comparison with the crystal structures of other ACE inhibitors and conclusions related to structure-activity relationships. J Med Chem 34:663-669.
13. Sakamoto Y, Sakamoto Y, Oonishi I, Ohmoto T. 1990. Conformation analysis of enalapril (MK-412) in solution by ^{1}H and ^{13}C NMR. J Mol Struct 238:25-224.
14. Ip DP, Brenner GS, Stevenson JM, Lindenbaum S, Douglas AW, Klein SD, McCauley JA.1986. High resolution spectroscopic evidence and solution calorimetry studies on the polymorphs of enalapril maleate. Int J Pharm 28:83-191.
15. Byrn SR, Pfeiffer RR, Stowell JG. 1999. Solid-State Chemistry of Drugs, 2nd edition. SSCI, Inc., West Lafayetter, Indiana, USA.
16. Haleblian J, McCrone W. 1969. Pharmaceutical applications of polymorphism. J Pharm Sci 58:911-929.
17. David WIF, Shankland K, Shankland N. 1998. Routine determination of molecular crystal structures from powder diffraction data. Chem Commun 931-932.
18. Engel GE, Wilke S, König O, Harris KDM, Leusen FJJ. 1999. PowderSolve- a complete package for crystal structure solution from powder diffraction patterns. J Appl Cryst 32:1169-1179.
19. Pagola S, Stephens PW. 2000. Towards the Solution of Organic Crystal Structures by Powder Diffraction. Materials Science Forum 321:40-45. Program and documentation available at http://powder.physics.sunysb.edu.
20. Dinnebier RE, Sieger P, Herbert N, Shankland K, David WIF. 2000. Structure characterization of three crystalline modifications of telmisartan by single crystal and high-resolution X-ray powder diffraction. J Pharm Sci 89:1465-1478.
21. Giovannini J, Perrin M-A, Louër D, Leveiller F. 2001. Ab initio crystal structure determination of three pharmaceutical compounds from x-ray powder diffraction data. Materials Science Forum 378-381:582-587.

22. Kariuki BM, Psallidas K, Harris KDM, Johnston RL, Lancaster RW, Staniforth SE, Cooper SM. 1999. Structure determination of a steroid directly from powder diffraction data. Chem Commun 1677-1678.
23. Tedesco E, Giron D, Pfeffer S. 2002. Crystal structure elucidation and morphology study of pharmaceuticals in development. CrytEngComm 4:393-400.
24. Smith EDL, Hammond RB, Jones MJ, Roberts KJ, Mitchell JBO, Price SL, Harris RK, Apperley DC, Cherryman JC, Docherty R. 2001. The determination of the crystal structure of anhydrous theophylline by x-ray powder diffraction with a systematic search algorithm, lattice energy calculations, and ^{13}C and ^{15}N solid-state NMR: a question of polymorphism in a given unit cell. J Phys Chem B 105:5818-5826.
25. Andreev YG, MacGlashan GS, Bruce PG. 1997. Ab initio solution of a complex crystal structure from powder-diffraction data using simulated-annealing method and a high degree of molecular flexibility. Phys Rev B 55:12011-12017.
26. Putz H, Cshon JC, Jansen M. 1999. Combined method for ab initio structure solution from powder diffraction data. J Appl Crystallogr 32:864-870.
27. Coelho AA. 2000. Whole-profile structure solution from powder diffraction data using simulated annealing. J Appl Crystallogr 33:899-908.
28. Pagola S, Stephens PW, Bohle DS, Kosar AD, Madsen SK. 2000. The structure of malaria pigment α-haematin. Nature 404:307-10.
29. Visser JW. 1969. A fully automatic program for finding the unit cell from powder data. J Appl Crystallogr 2:89-95.
30. Material Studio. Accelrys Inc. 2001. San Deigo, CA, USA.
31. Larson AC, von Dreele RB. 2000. GSAS: General Structure Analysis System. Los Alamos National Laboratory. Report LAUR 86-748.
32. Cerius^2. Computer Simulation Software Package. Accelrys Inc. 2001. San Deigo, CA, USA.
33. Mayo SL, Olafson BD, Goddard WA III. 1990. DREDING: a generic force filed for molecular simulations. J Phys Chem 94:8897-8909.

34. Buttar D, Charlton MH, Docherty R, Starbuck J. 1998. Theoretical investigations of conformational aspects of polymorphism. Part 1: o-acetamidobenzamide. J Chem Soc, Perkin Trans 2 763-772.
35. Payne RS, Roberts RJ, Rowe RC, Docherty R. 1999. Examples of successful crystal structure prediction: polymorphs of primidone and progesterone. Int J Pharm 177:231-245.
36. Roberts RJ, Payne RS, Rowe RC. 2000. Mechanical property predictions for polymorphs of sulphathiazole and carbamazepine. Eur J Pharm Sci 9:277-283.
37. Frisch MJ, Trucks GW, Schlegel HB, Gill PMW, Johnson BG, Wong MW, Foresman JB, Robb MA, Head-Gordan M, Replogle ES, Gomperts R, Andres JL, Raghavachari K, Binkley JS, Gonzalez C, Martin RL, Fox DJ, Defrees DJ, Baker J, Stewart JJP., Pople JA, 1993. Gaussian 92/DFT, Revision G.1. Gaussian Inc. Pittsburgh, PA, USA.
38. Kitaigoroskii AI. 1961. Organic Chemical Crystallography. Consultant Bureau, New York, NY, USA.

Figure Captions

Figure 1. XRD patterns of enalapril maleate (a) Form I and (b) Form II. Data were taken on a laboratory diffractometer using Cu $K_\alpha 1$ radiation.

Figure 2. Solid state 13C NMR spectra of enalapril maleate (a) Form I and (b) Form II. The resonances marked with asterisks are sidebands.

Figure 3. Final Rietveld plot of enalapril maleate Form II. (observed: +, calculated, -, and difference: bottom)

Figure 4. Stereoview of crystal structure enalapril maleate Form II. Hydrogen bonding is represented by dashed line.

Figure 5. Viewing down a 2-fold screw axis of enalapril maleate (a) Form I and (b) Form II. Carbon atoms are shown in green, nitrogen in yellow and oxygen in red. Hydrogen atoms are removed for clarity.

Figure 6. Infrared spectra of enalapril maleate (a) Form I and (b) Form II showing the range 900 to 600 cm^{-1}.

Figure 7. Solid-state ^{13}C NMR of enalapril maleate (a) Form I and (b) Form II showing the range 110 to 160 ppm.

Figure 8. Solid-state ^{13}C NMR of enalapril maleate (a) Form I and (b) Form II showing the range 0 to 40 ppm.

Figure 9. The conformation of enalapril in (a) Form I along with atom numbering, and in (b) Form II.

Table 1. Degrees of Freedom and *R*wp Factors in Each MC/SA Search Cycle

MC/SA	torsion		translation+rotation		DOF	*R*wp
	enalapril	maleate	enalapril	maleate		%
1	fixed	fixed	refined	refined	12	17.51
2	refined	fixed	fixed	fixed	11	14.04
3	fixed	fixed	refined	refined	12	13.69
4	fixed	refined	fixed	refined	8	13.66

Table 2. Crystal Data and Structure Refinement for the Form II

Empirical Formula	$C_{24}H_{32}N_2O_9$
Temperature (K)	297
Crystal System	Orthorhombic
Space Group	$P2_12_12_1$
a (Å)	33.9898(3)
b (Å)	11.2109(1)
c (Å)	6.64195(3)
V (Å)^3	2530.96(5)
Z	4
Calculated density (g/cm^3)	1.29
Profile function	Pseudo-Voigt
Scan range ($^o2\theta$)	2.0-47.65
Step size ($^o2\theta$)	0.005
Counting time/step (s)	2.0-17.0
Wavelength (Å)	1.1508
Number of data points	88000
Number of parameters refined	122
*R*wp	0.0761
χ^2	31.1

Table 3. Fractional Atomic Coordinates and Equivalent Isotropic Displacement Parameters for the Form II[a]

	x	y	z	*U*iso
C1	0.7161(4)	0.3362(12)	-0.0364(19)	0.0441(8)
C2	0.7017(4)	-0.2149(11)	0.0440(2)	0.0441(8)
N3	0.7183(3)	-0.2180(10)	0.2417(19)	0.0441(8)
C4	0.7449(4)	-0.3204(13)	0.2742(20)	0.0441(8)
C5	0.7519(4)	-0.3733(10)	0.0675(22)	0.0441(8)
C6	0.7800(3)	-0.2749(12)	0.3683(22)	0.0441(8)
O7	0.8002(2)	-0.1768(8)	0.3246(12)	0.0441(8)
O8	0.7982(2)	-0.3400(8)	0.5059(12)	0.0441(8)
C9	0.7032(3)	-0.1414(13)	0.3960(19)	0.0441(8)
O10	0.7243(3)	-0.1537(8)	0.5770(12)	0.0441(8)
C11	0.6696(4)	-0.0476(12)	0.3537(21)	0.0441(8)
C12	0.6984(3)	0.0606(11)	0.2758(18)	0.0441(8)
N13	0.6589(2)	-0.0247(10)	0.5690(18)	0.0441(8)
C14	0.6305(4)	0.0687(11)	0.5458(24)	0.0441(8)
C15	0.6167(4)	0.1017(12)	0.7617(21)	0.0441(8)
O16	0.6208(2)	0.0355(7)	0.9225(12)	0.0441(8)
O17	0.5932(2)	0.2022(8)	0.7932(13)	0.0441(8)
C18	0.5718(4)	0.2320(10)	0.9863(19)	0.0441(8)
C19	0.5335(4)	0.1724(11)	0.9769(18)	0.0441(8)
C20	0.5938(4)	0.0514(12)	0.4097(19)	0.0441(8)
C21	0.5655(3)	-0.0472(11)	0.4955(20)	0.0441(8)
C22	0.5341(4)	-0.0740(14)	0.3477(23)	0.0441(8)
C23	0.4996(5)	-0.0071(12)	0.3717(19)	0.0441(8)
C24	0.4677(4)	-0.0337(12)	0.1934(26)	0.0441(8)
C25	0.4794(4)	-0.1024(12)	0.0282(22)	0.0441(8)
C26	0.5113(5)	-0.1707(12)	0.0396(21)	0.0441(8)
C27	0.5418(4)	-0.1410(13)	0.1638(26)	0.0441(8)
C28	0.3701(5)	1.0488(11)	1.8396(18)	0.0542(14)
C29	0.3649(5)	1.1683(12)	1.9105(18)	0.0542(14)
O30	0.3682(3)	1.2621(6)	1.7808(12)	0.0542(14)
O31	0.3681(3)	1.2054(8)	2.0984(13)	0.0542(14)
C32	0.3643(5)	0.9489(11)	1.9198(20)	0.0542(14)
C33	0.3582(5)	0.9184(11)	2.1378(21)	0.0542(14)
O34	0.3525(3)	0.8142(7)	2.2096(13)	0.0542(14)
O35	0.3642(3)	1.0115(8)	2.2671(13)	0.0542(14)

a) Numbers in parentheses are statistical esd's from the Rietveld program. It is widely known that realistic error estimates from powder experiments are substantially larger than these numbers, perhaps a factor of ten.

Table 4. Selective Torsion Angles of Enalapril

Torsion angle	Form I(º)	Form II(º)
C15-O17-C18-C19	-166.7	-87.5
C27-C22-C21-C20	83.9	72.9
C22-C21-C20-C14	179.4	-171.6
C21-C20-C14-N13	67.7	65.5
C20-C14-N13-C11	57.7	55.7
ϕ1 (C9-C11-N13-C14)	175.0	175.0
ψ1 (N3-C9-C11-N13)	156.3	164.1
ω (C4-N3-C9-C11)	-178	-179
ϕ2 (C6-C4-N3-C9)	-52.8	-59.2
ψ2 (O8-C6-C4-N3)	139.7	143.7

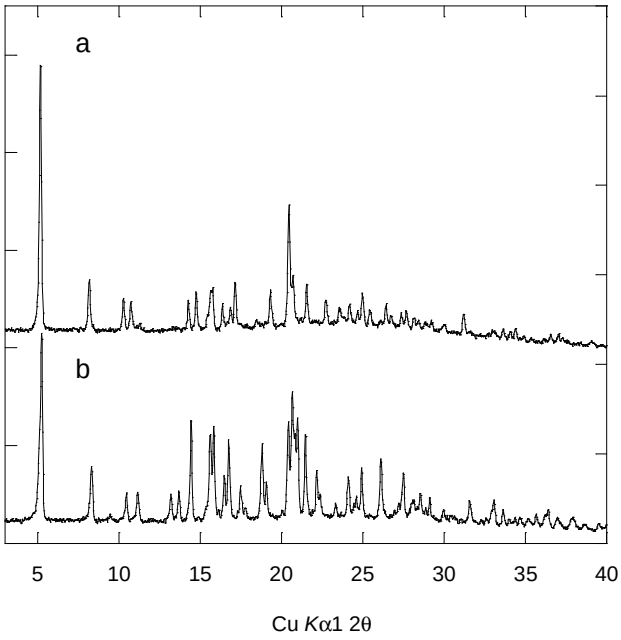

Figure 1

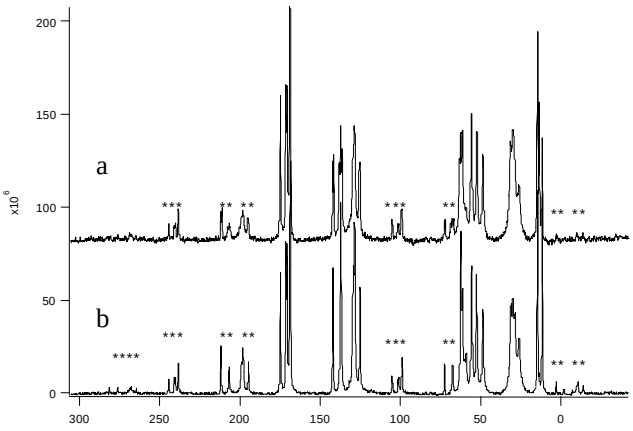

Figure 2

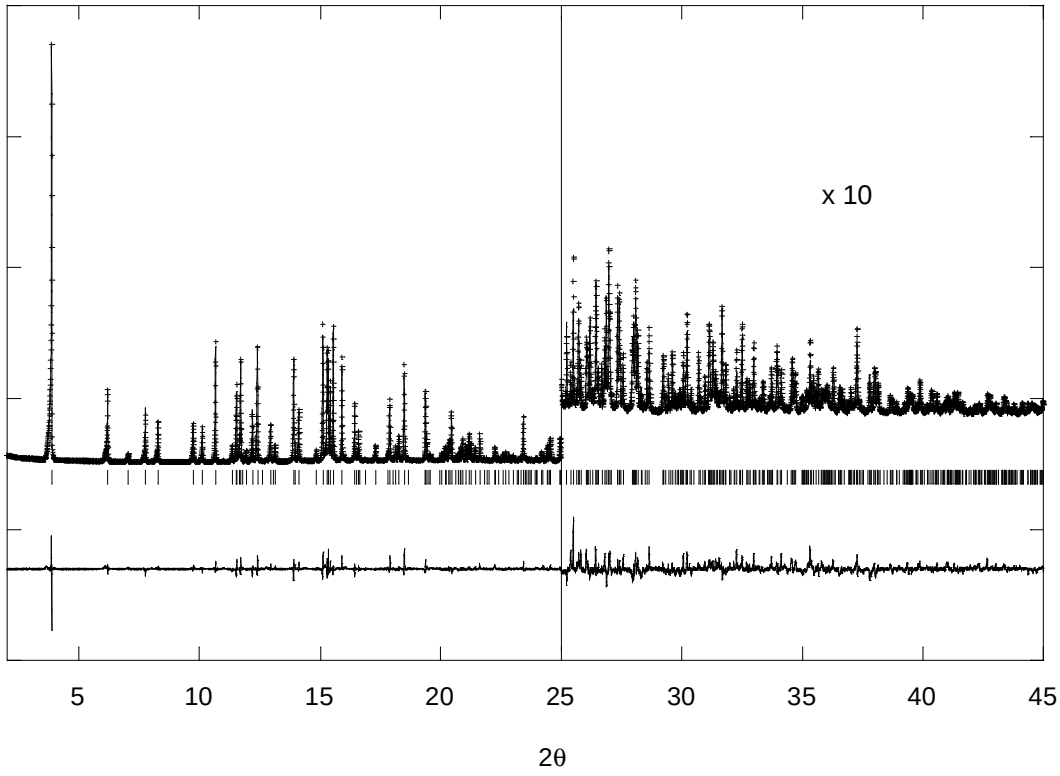

Figure 3

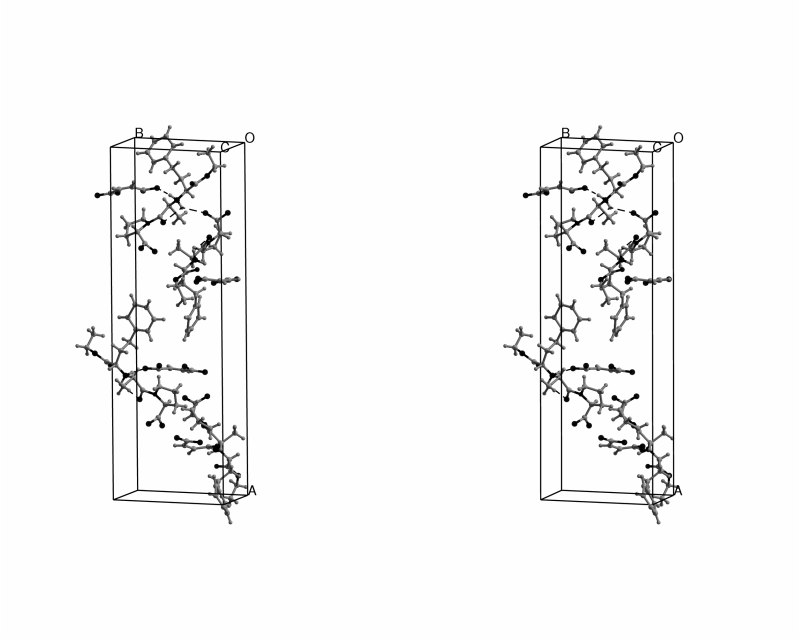

Figure 4

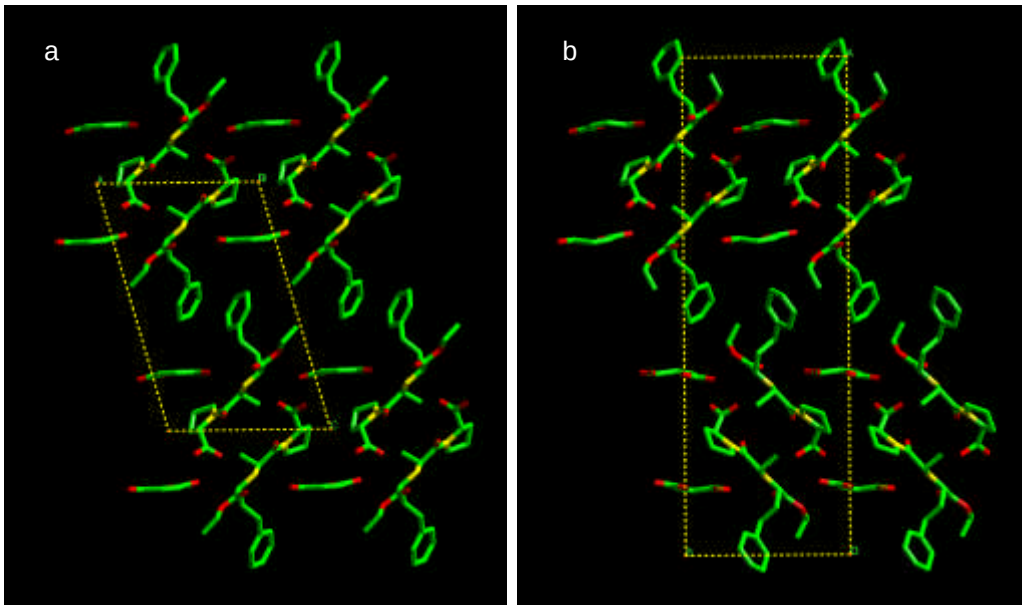

Figure 5

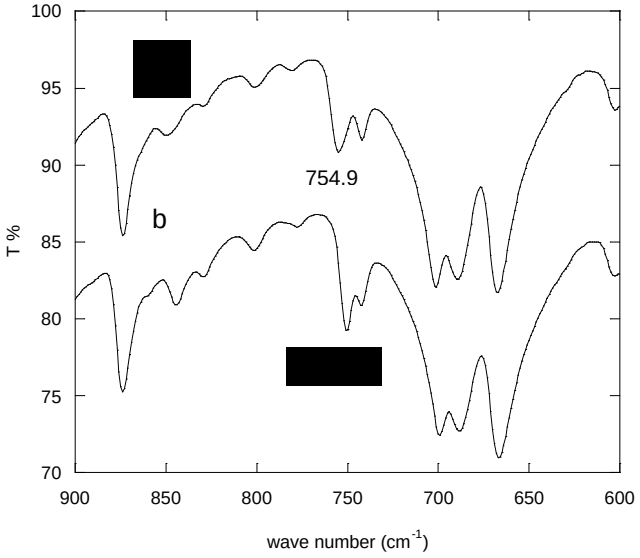
100
95
90
85
80
75
70
T %
754.9
b
900
850
800
750
700
650
600
wave number (cm-1)

Figure 6

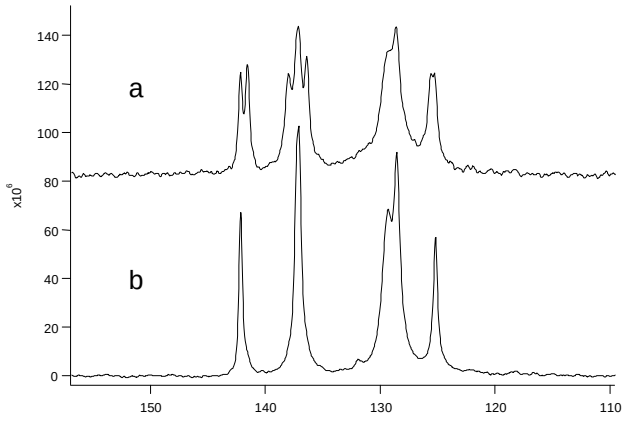

Figure 7

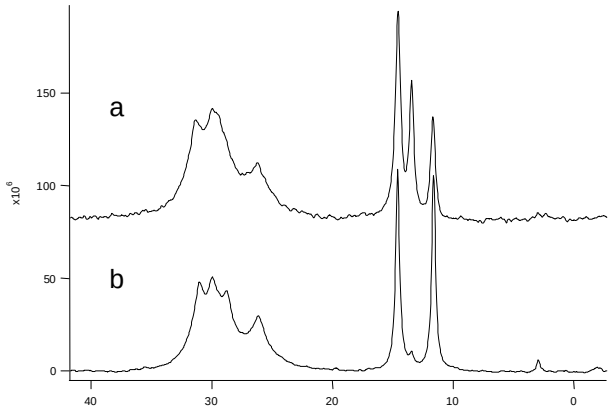

Figure 8

a

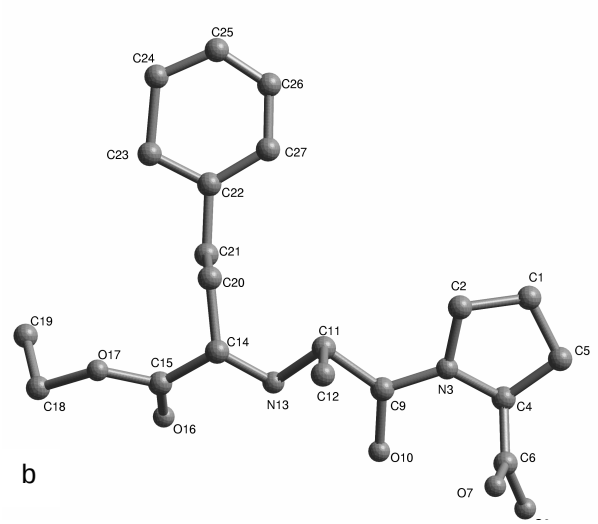
C25
C24
C26
C23
C27
C22
C21
C20
C2
C1
C19
C11
C14
C5
O17
C15
N3
C18
N13
C12
C9
C4
O16
O10
C6
O7
b

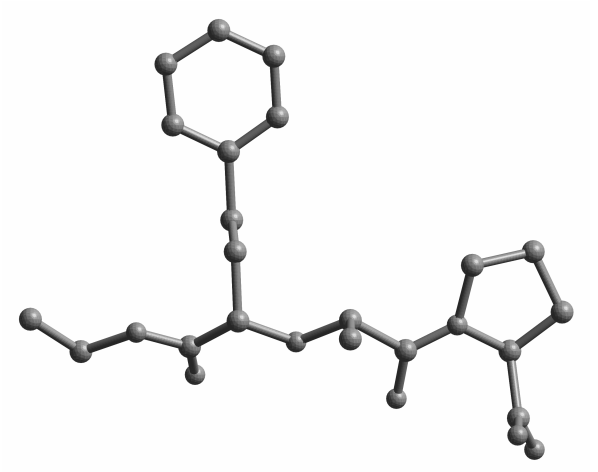

Figure 9